Tunneling characteristics in chemical vapor deposited graphene–hexagonal boron nitride–graphene junctions

T. Roy, L. Liu, S. de la Barrera, B. Chakrabarti, Z. R. Hesabi, C. A. Joiner, R. M. Feenstra, G. Gu, and E. M. Vogel

---

Articles you may be interested in

Interlayer coupling enhancement in graphene/hexagonal boron nitride heterostructures by intercalated defects or vacancies
J. Chem. Phys. **140**, 134706 (2014); 10.1063/1.4870097

Thermal interface conductance across a graphene/hexagonal boron nitride heterojunction
Appl. Phys. Lett. **104**, 081908 (2014); 10.1063/1.4866335

Field-effect control of tunneling barrier height by exploiting graphene's low density of states
J. Appl. Phys. **113**, 136502 (2013); 10.1063/1.4795542

In-plane and tunneling pressure sensors based on graphene/hexagonal boron nitride heterostructures
Appl. Phys. Lett. **99**, 133109 (2011); 10.1063/1.3643899

Chemical vapor deposition-assembled graphene field-effect transistor on hexagonal boron nitride
Appl. Phys. Lett. **98**, 262103 (2011); 10.1063/1.3604012

Tunneling characteristics in chemical vapor deposited graphene–hexagonal boron nitride–graphene junctions

T. Roy,[1] L. Liu,[2] S. de la Barrera,[3] B. Chakrabarti,[1,4] Z. R. Hesabi,[1] C. A. Joiner,[1] R. M. Feenstra,[3] G. Gu,[2] and E. M. Vogel[1]

[1]*School of Materials Science and Engineering, Georgia Institute of Technology, 771 Ferst Drive, Atlanta, Georgia 30332, USA*
[2]*Department of Electrical Engineering and Computer Science, University of Tennessee, 1520 Middle Drive, Knoxville, Tennessee 37996, USA*
[3]*Department of Physics, Carnegie Mellon University, 5000 Forbes Ave., Pittsburgh, Pennsylvania 15213, USA*
[4]*Department of Materials Science and Engineering, University of Texas at Dallas, 800 West Campbell Rd., Richardson, Texas 75080, USA*

Large area chemical vapor deposited graphene and hexagonal boron nitride was used to fabricate graphene–hexagonal boron nitride–graphene symmetric field effect transistors. Gate control of the tunneling characteristics is observed similar to previously reported results for exfoliated graphene–hexagonal boron nitride–graphene devices. Density-of-states features are observed in the tunneling characteristics of the devices, although without large resonant peaks that would arise from lateral momentum conservation. The lack of distinct resonant behavior is attributed to disorder in the devices, and a possible source of the disorder is discussed. © 2014 AIP Publishing LLC.
[http://dx.doi.org/10.1063/1.4870073]

Graphene is considered a promising candidate for future electronic devices owing to the high mobility of its carriers, linear dispersion, and perfect two-dimensional (2D) confinement. However, monolayer graphene-based transistors have a low switching ratio owing to the semi-metallic nature of graphene.[1] Graphene-insulator-graphene symmetric field effect transistors (SymFETs), where a bottom gate controls the carriers in the bottom layer graphene while a top gate controls the top graphene layer, have been theoretically shown to exhibit negative differential resistance (NDR) in the tunneling characteristics, due to resonance in tunneling when the Dirac points of the two graphene layers are aligned.[2,3] Britnell *et al.* first demonstrated gate-controlled tunneling in exfoliated graphene–hexagonal boron nitride (h-BN)–graphene heterostructures[4,5] and later demonstrated resonant tunneling induced NDR in a similar structure.[6] It has also theoretically been shown that the resonance peak is largely dependent on the degree of defect-induced disorder and may also depend on the misorientation of the two graphene layers.[2,3,6] Although an exfoliated graphene-based system allows the observation of NDR, the large scale realization of these devices is not possible. In this work, SymFETs with both graphene and h-BN grown by chemical vapor deposition (CVD) have been fabricated and characterized.

Figure 1 shows the structure of a graphene–h-BN–graphene SymFET. CVD graphene obtained from ACS Material[7] was transferred onto 90-nm-thick SiO$_2$ on a silicon substrate using wet transfer techniques, and then annealed in forming gas.[8] After patterning the graphene by etching in O$_2$ plasma, Ni/Au contacts were deposited on this bottom layer of graphene. A 2-nm-thick Ti layer was deposited using e-beam evaporation, and then wet-etched to form a Ti protection layer. Hexagonal boron nitride was grown on Ni using atmospheric CVD in a hot wall furnace. Nickel foils (25 μm, 99.5%, Alfa Aesar) were chosen as the catalytic substrates for

the h-BN synthesis. Ammonia borane (BH$_3$-HN$_3$), a commonly used h-BN precursor, was heated to sublime at ~120 °C by a heating tape and delivered to the furnace by Ar:H$_2$ carrier gas. The typical growth time is 10 min, followed by rapid cooling. The growth process results in multilayer h-BN with 3–7 layers, identified by TEM cross-section characterization. The h-BN was wet-transferred and annealed in forming gas, the Ni being etched using FeCl$_3$ solution and dilute HCl. Next, CVD graphene was wet-transferred as the top layer. The top graphene was then patterned by etching with O$_2$ plasma to a dimension of 49 μm × 13 μm. The h-BN layers are also etched in the plasma, while the Ti layer protects the bottom graphene layer. Ni/Au contacts were deposited on the top graphene layer. The structures thus formed were again annealed in forming gas. A 2-nm-thick Ti seeding layer is deposited, followed by atomic layer deposition of ~10 nm HfO$_2$. Ni/Au is deposited as top gate contacts. Fig. 1(b) shows the cross-section of the device, with the biasing scheme. The bottom gate primarily controls the carrier concentration in the bottom layer, while the top gate primarily controls the top graphene layer. The Dirac points of the two layers are adjusted by the voltage across the tunnel barrier, V_{DS}.

Figure 2 shows typical characteristics of tunnel current density (J_D) on a logarithmic scale versus voltage for temperatures of 77 K and 300 K. We find that the tunneling current is not dependent on temperature. This indicates that direct tunneling current through the h-BN dominates any trap-assisted tunneling current. In contrast, for the case of thick dielectrics with a high defect density, the current flowing through the dielectric is trap-assisted, resulting in temperature-dependent tunnel current characteristics.[9]

Figure 3 shows experimental current density on a logarithmic scale versus voltage for three typical CVD graphene–h-BN–graphene devices taken across a die that is
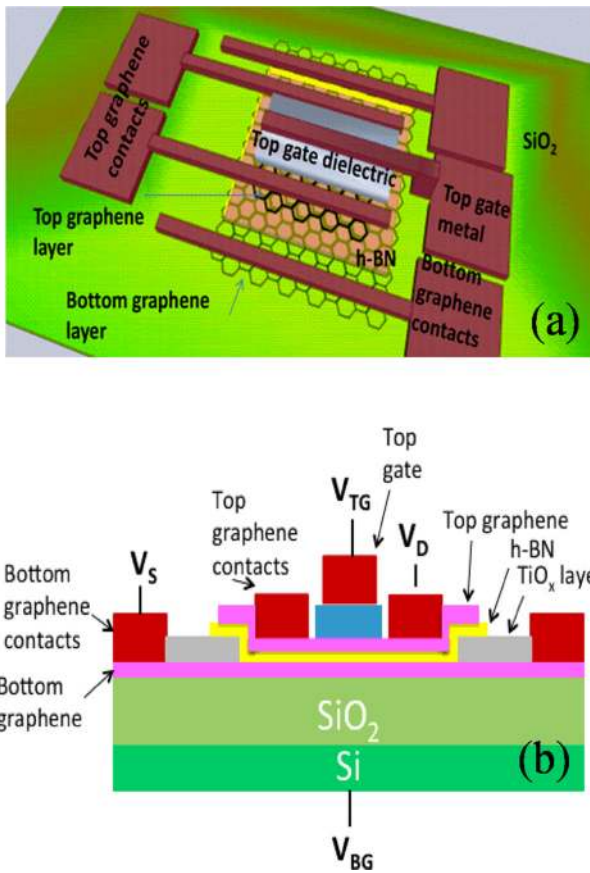
FIG. 1. (a) Structure of a graphene–h-BN–graphene transistor. (b) Cross-sectional view of the device with the biasing scheme. (Not to scale.)

$\sim$1 cm^2. Also shown in Fig. 3 are experimental characteristics for similar heterostructures fabricated using exfoliated graphene and exfoliated h-BN of either four[4] or six[5] layers. The magnitude of current density through exfoliated h-BN has previously been observed to change by $\sim$20$\times$ per monolayer of h-BN.[4] Comparing the magnitude of the current density for the CVD case to that of exfoliated suggests the thickness of the multilayer CVD h-BN ranges from approximately 4 to 5 monolayers. We also note that the shape of the characteristics as a function of the voltage across the graphene electrodes is very similar.
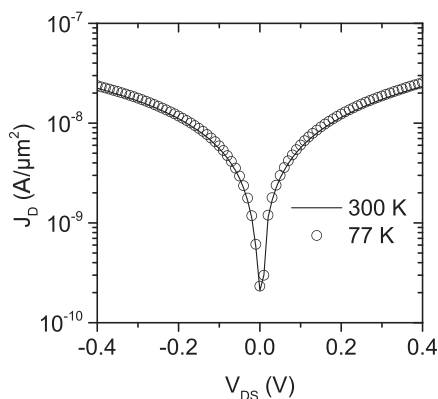

FIG. 2. Experimental current-voltage characteristics ($V_{BG} = V_{TG} = 0$ V) indicating temperature-independent (direct) tunneling for the CVD graphene–h-BN–graphene structure. All of the measured devices show similar, temperature-independent, behavior.
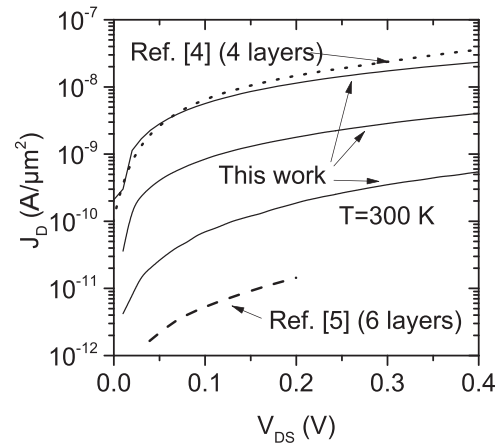

FIG. 3. Experimental current-voltage characteristics ($V_{BG} = V_{TG} = 0$ V) for three CVD graphene–h-BN–graphene devices taken from across one sample. Measured results from the literature[4,5] for exfoliated graphene–h-BN–graphene devices are shown for comparison. The results suggest that our multilayer CVD h-BN has 4 to 5 layers with a variation of approximately 1 layer.

Figure 4 shows typical characteristics of tunnel current density on logarithmic scale versus voltage across the graphene electrodes, for various back gate voltages. Also shown in Fig. 4 are current-voltage characteristics for various back gate voltages for similar heterostructures with six exfoliated h-BN layers.[5] The results demonstrate gate-controlled tunneling for CVD graphene–h-BN–graphene devices similar to the previously reported results for exfoliated graphene–h-BN–graphene.

When examined over a *linear* current range, some devices show plateaus and/or kinks in their current-voltage characteristic, as shown in Fig. 5(a). The plateaus in the curves are indicated with a red circle. To understand this behavior we perform simulations of the device behavior, using the theory[5] in which *no in-plane momentum conservation* is assumed.[14] The resulting simulated characteristics are shown in Fig. 5(b), for precisely the same device geometry (i.e.,
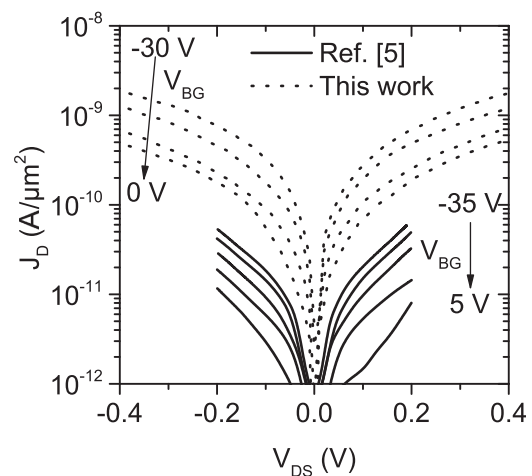

FIG. 4. Experimental current-voltage characteristics on a logarithmic scale for various V_{BG} ($V_{TG} = 0$ V) for one CVD graphene–h-BN–graphene device ($\sim$5 h-BN layers). A measured result from the literature for an exfoliated graphene–h-BN–graphene device (4 h-BN layers) is shown for comparison.[5] Similar control of the tunneling characteristics by the applied back gate voltage is observed.

tunnel barrier and gate dielectric thicknesses) as in the experiment, and assuming slight p-doping in the graphene layers ($\Delta = -0.1$ eV is the separation of the Fermi energy and Dirac point for both layers, for zero V_{DS}). We find good agreement between the simulated and the experimental results. The plateau in the curves arises when the Fermi energy of one of the graphene layers (the bottom graphene layer in this case) passes through a minimum in the density-of-states, i.e., the Dirac point for that electrode. Over this small energy range, the transmission probability of the carriers is approximately constant whereas the density of carriers available for tunneling decreases and then increases, resulting in the plateau.

Our results indicate that we have well-defined tunneling occurring between the two graphene electrodes, with clear modulation due to the bottom gate. However, we obtain agreement between the simulated and measured tunneling characteristics only when we consider the situation of no in-plane momentum conservation. When some limited amount of momentum conservation is included in a rigorous transfer Hamiltonian computation, then a *resonant peak* occurs in the tunneling current,[2,3,6] but we observe no such peak in our experimental characteristics (even when measured over a larger range than that of Fig. 4). The plateau discussed above does
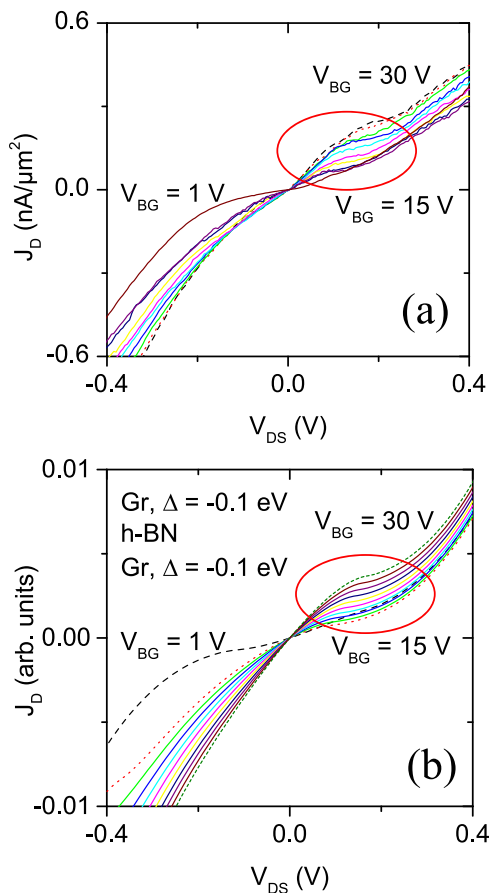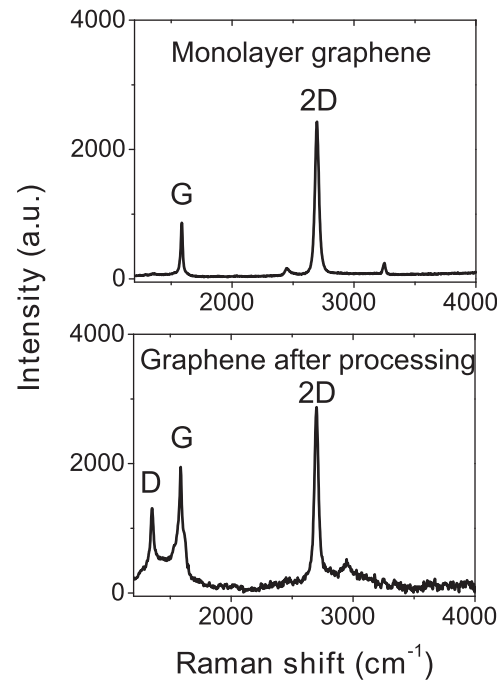

FIG. 6. Raman spectra of (a) monolayer graphene transferred onto the SiO$_2$ substrate, (b) the same graphene after processing and transfer of the h-BN. The processing or h-BN transfer has resulted in an enhanced D-peak indicating disorder.

not indicate the occurrence of a resonant peak, but rather, is simply a density-of-states effect.[5] A complete lack of resonant behavior corresponds to a *lateral coherence length* for the tunneling of $\lesssim 1$ nm in the transfer Hamiltonian approach,[2] which produces results that are nearly identical with those from the non-momentum-conserving theory.

Fig. 6(a) shows the Raman spectrum of that graphene layer, with 2D/G ratio of $\sim$2:1 and no D peak. This demonstrates that the bottom layer of graphene is single monolayer and the defect density is quite low.[10] However, following Ti deposition and removal, along with transfer of the h-BN onto the bottom graphene layer, we find that its characteristics are degraded (Fig. 6(b). The latter displays a peak $\sim$1360 cm^{-1} which we associate with the disorder (D) peak of graphene. (This Raman line is at nearly the same energy as that due to the E$_{2g}$ vibrational mode within the h-BN layers. However, the concomitant increase in width of the graphene G peak between Figs. 6(a) and 6(b) indicates that the 1360 cm^{-1} peak does, indeed, arise from the D line of graphene.[11,12] Furthermore, a shoulder appears on the right side of the G peak, indicating the defect induced D′ mode.[13]) Apparently, the processing steps of Ti deposition/removal followed by h-BN transfer have produced disorder in the bottom graphene layer. Therefore, in our devices, we attribute the small coherence length to the bottom graphene layer which has suffered degradation due to the full device fabrication. Further examination of these process steps will, we believe, reveal the limiting step that produces the degradation of the bottom graphene layer in the present devices.

In conclusion, we have demonstrated gate-controlled tunneling in a CVD graphene–h-BN–graphene system similar to the exfoliated system.[4,5] Temperature-independent tunneling is found, indicating non-trap-assisted direct

FIG. 5. (a) Experimental current-voltage characteristics on a linear scale for various V_{BG} (T = 300 K, V_{TG} = 0 V) for one CVD graphene–h-BN–graphene device ($\sim$5 h-BN layers). A "plateau region" is highlighted by the red circle. (b) Simulated tunneling characteristic of a graphene–h-BN–graphene device, for the same device parameters as (a), for the situation of no in-plane momentum conservation.

tunneling. Density-of-states features are observed in the characteristics, in excellent consistence with simulation, which clearly reveals the role of defects on possible resonant tunneling or the lack thereof. Improvements in the processing steps will therefore lead to higher crystalline order in both graphene layers, thereby achieving resonant behavior and the associated NDR. With such improvements, practical applications of these devices in large scale electronic circuits should be possible.

[1]F. Schwierz, Nat. Nanotechnol. **5**, 487 (2010).
[2]R. M. Feenstra, D. Jena, and G. Gu, J. Appl. Phys. **111**, 043711 (2012).
[3]P. Zhao, R. M. Feenstra, G. Gong, and D. Jena, IEEE Trans. Electron Devices **60**, 951 (2013).
[4]L. Britnell, R. V. Gorbachev, R. Jalil, B. D. Belle, F. Schedin, M. I. Katsnelson, L. Eaves, S. V. Morozov, A. S. Mayorov, N. M. R. Peres, A. H. C. Neto, J. Leist, A. K. Geim, L. A. Ponomarenko, and K. S. Novoselov, Nano Lett. **12**, 1707 (2012).
[5]L. Britnell, R. V. Gorbachev, R. Jalil, B. D. Belle, F. Schedin, A. Mishchenko, T. Georgiou, M. I. Katsnelson, L. Eaves, S. V. Morozov, N. M. R. Peres, J. Leist, A. K. Geim, K. S. Novoselov, and L. A. Ponomarenko, Science **335**, 947 (2012).
[6]L. Britnell, R. V. Gorbachev, A. K. Geim, L. A. Ponomarenko, A. Mishchenko, M. T. Greenaway, T. M. Fromhold, K. S. Novoselov, and L. Eaves, Nat. Commun. **4**, 1794 (2013).
[7]ACS Material, *Technical Data Sheet ACS Material Graphene/Cu* (ACS Material, 2013).
[8]J. Chan, A. Venugopal, A. Pirkle, S. McDonnell, D. Hinojos, C. W. Magnuson, R. S. Ruoff, L. Colombo, R. M. Wallace, and E. M. Vogel, ACS Nano **6**, 3224 (2012).
[9]T. Roy, Z. R. Hesabi, C. A. Joiner, A. Fujimoto, and E. M. Vogel, Microelectron. Eng. **109**, 117 (2013).
[10]A. C. Ferrari, J. C. Meyer, V. Scardaci, C. Casiraghi, M. Lazzeri, F. Mauri, S. Piscanec, D. Jiang, K. S. Novoselov, S. Roth, and A. K. Geim, Phys. Rev. Lett. **97**, 187401 (2006).
[11]R. V. Gorbachev, I. Riaz, R. R. Nair, R. Jalil, L. Britnell, B. D. Belle, E. W. Hill, K. S. Novoselov, K. Watanabe, T. Taniguchi, A. K. Geim, and P. Blake, Small **7**, 465 (2011).
[12]L. Song, L. Ci, H. Lu, P. B. Sorokin, C. Jin, J. Ni, A. G. Kvashnin, D. G. Kvashnin, J. Lou, B. I. Yakobson, and P. M. Ajayan, Nano Lett. **10**, 3209 (2010).
[13]M. S. Dresselhaus, A. Jorio, M. Hoffmann, G. Dresselhaus, and R. Saito, Nano Lett. **10**, 751 (2010).
[14]Our computations assume a valence band offset between BN and graphene of 3 eV, rather than the 1.5 eV of Ref. 5. The results are weakly dependent on this value.